Efficient stacking of *iso*-butene in sulfonate functional metal-organic frameworks for efficient *iso*-butene/*iso*-butane separation

Zhensong Qiu,[†a] Jiyu Cui,[†a] Dengzhuo Zhou,[a] Zhenglu Yang,[ab] Xiaofei Lu,[b] Xian Suo,[b] Anyun Zhang,[a] Xili Cui,[ab] Lifeng Yang,*[ac] Huabin Xing*[ab]

[a.] *Key Laboratory of Biomass Chemical Engineering of Ministry of Education, College of Chemical and Biological Engineering, Zhejiang University, Hangzhou, Zhejiang 310027, PR China.*

[b.] *ZJU-Hangzhou Global Scientific and Technological Innovation Center, Hangzhou 311215, China.*

[c.] *State Key Laboratory of Silicon Materials, School of Materials Science and Engineering, Zhejiang University, Hangzhou 310027, China.*

† These authors contributed equally.

** Corresponding author: lifeng_yang@zju.edu.cn, xinghb@zju.edu.cn*

Electronic Supplementary Information (ESI) available: [additional figures, crystal information]. See DOI: 10.1039/x0xx00000x

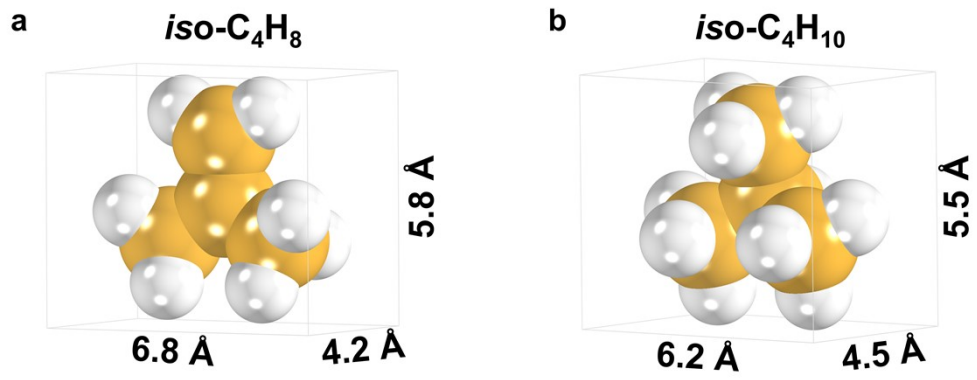

Fig. S1. Molecular dimensions of (a) *iso*-C_4H_8 and (b) *iso*-C_4H_{10}

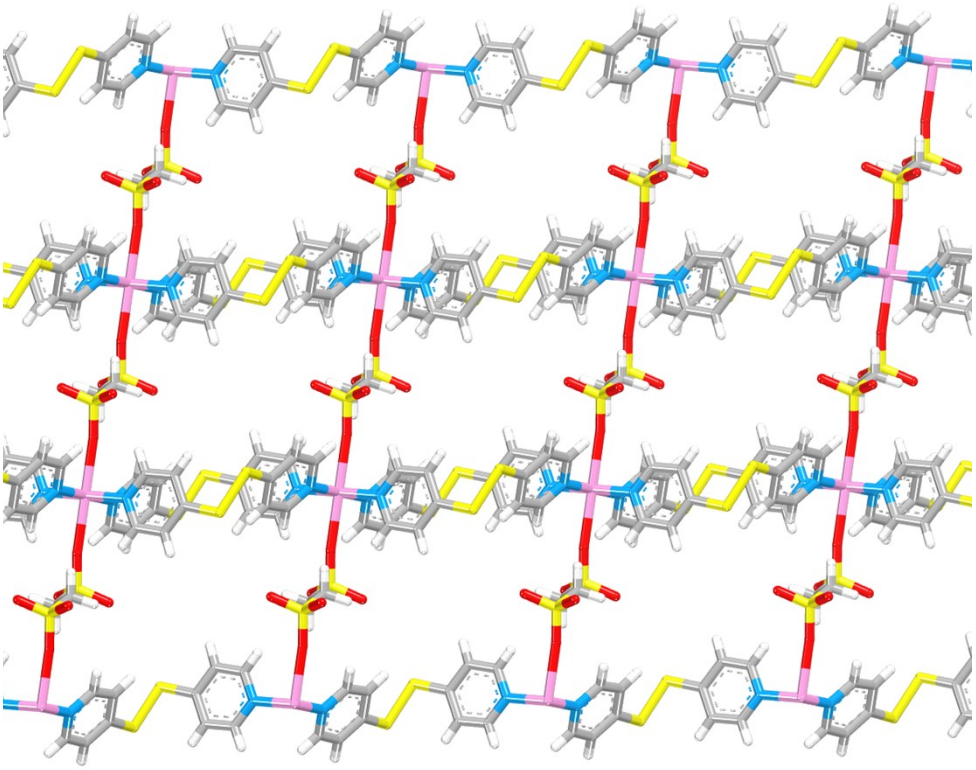

Fig. S2. Illustration of the 2D coordination network of ZU-603

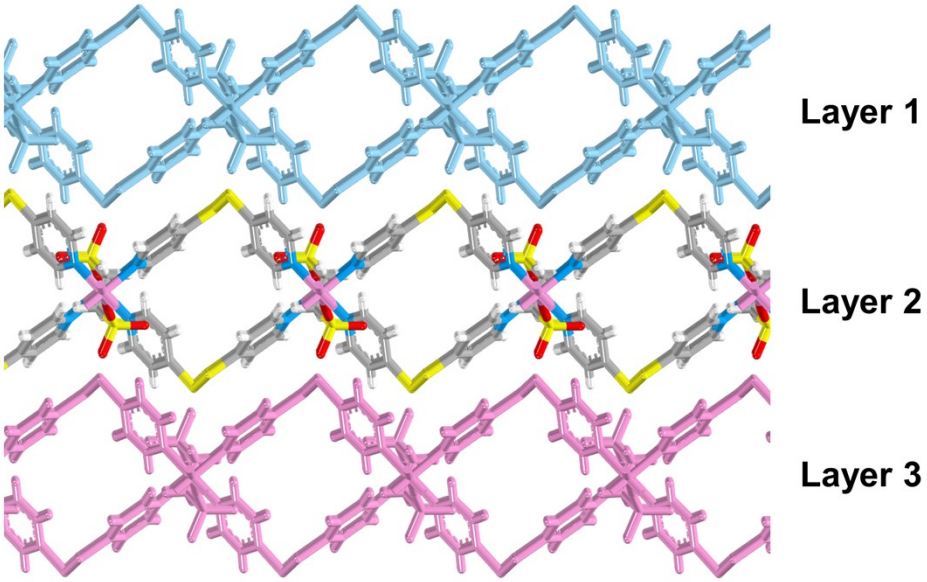

Fig. S3. Illustration of the 2D layered structure of ZU-603. (Different colors are used to represent different layers for clarity)

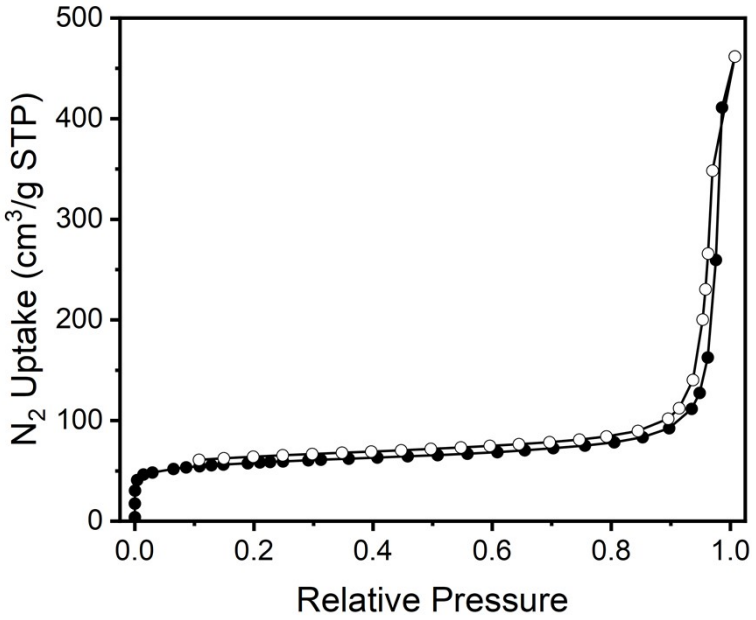

Fig. S4. N_2 adsorption and desorption isotherms of ZU-603 at 77 K

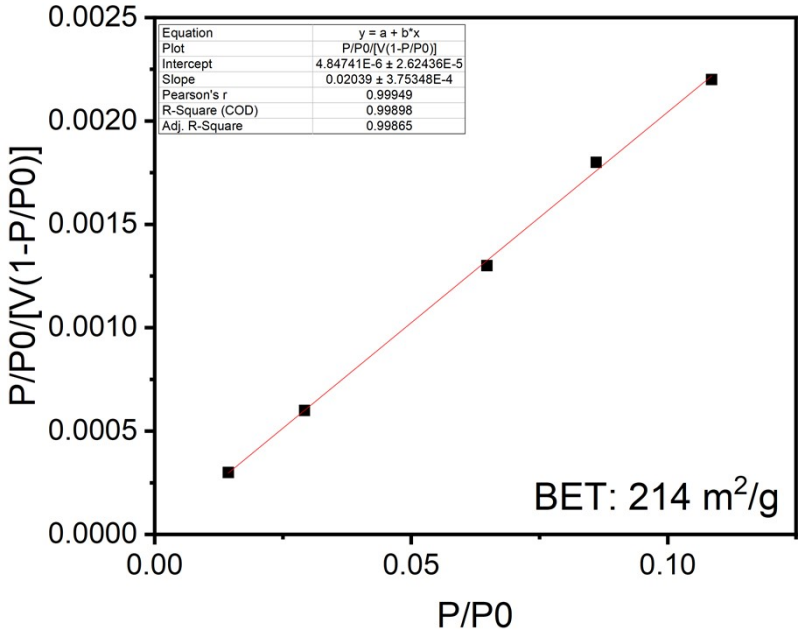

Fig. S5. BET calculation of ZU-603 using the N_2 adsorption isotherm at 77 K.

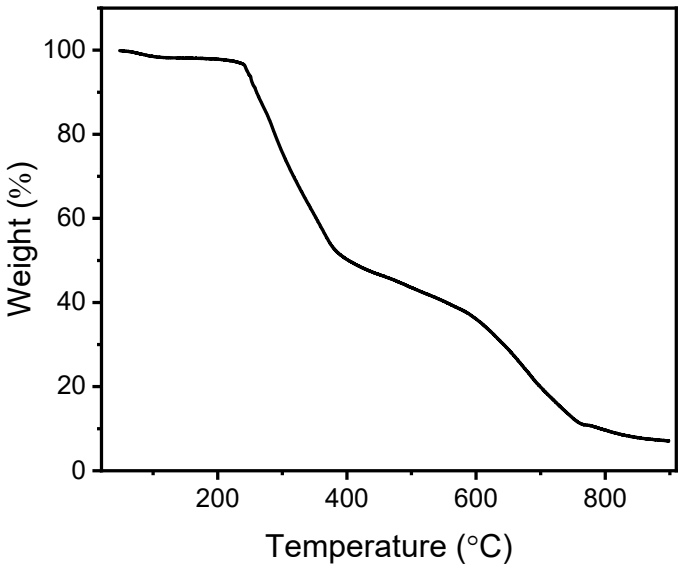

Fig. S6. Thermogravimetric analysis of ZU-603 under nitrogen flow (50-900°C, 10°C min^{-1}).

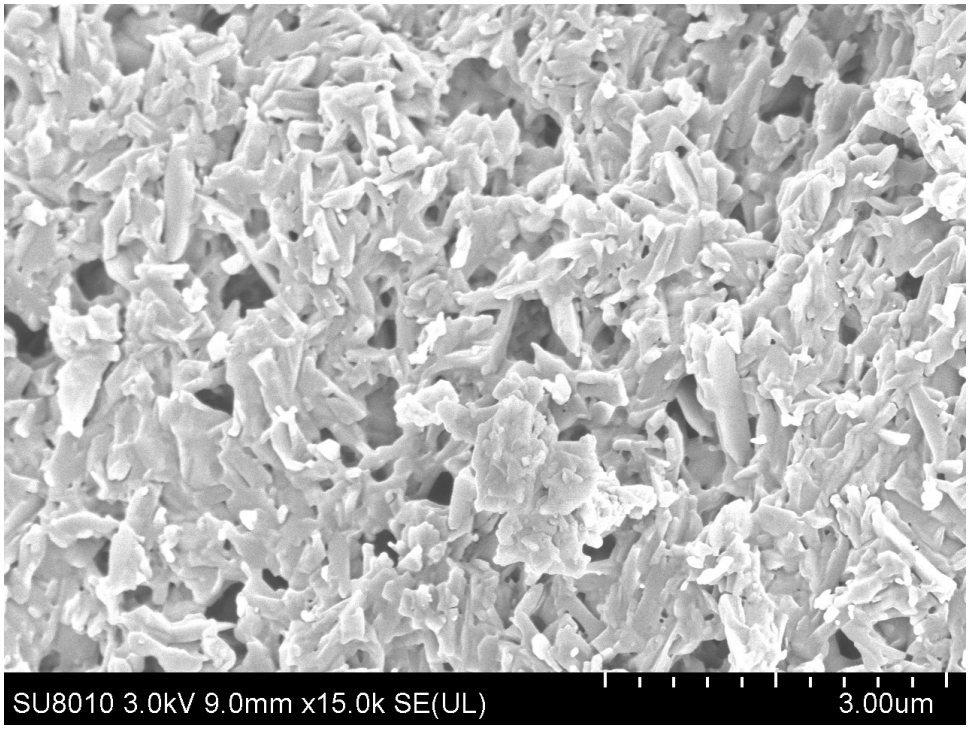

Fig. S7. SEM image of ZU-603 particles.

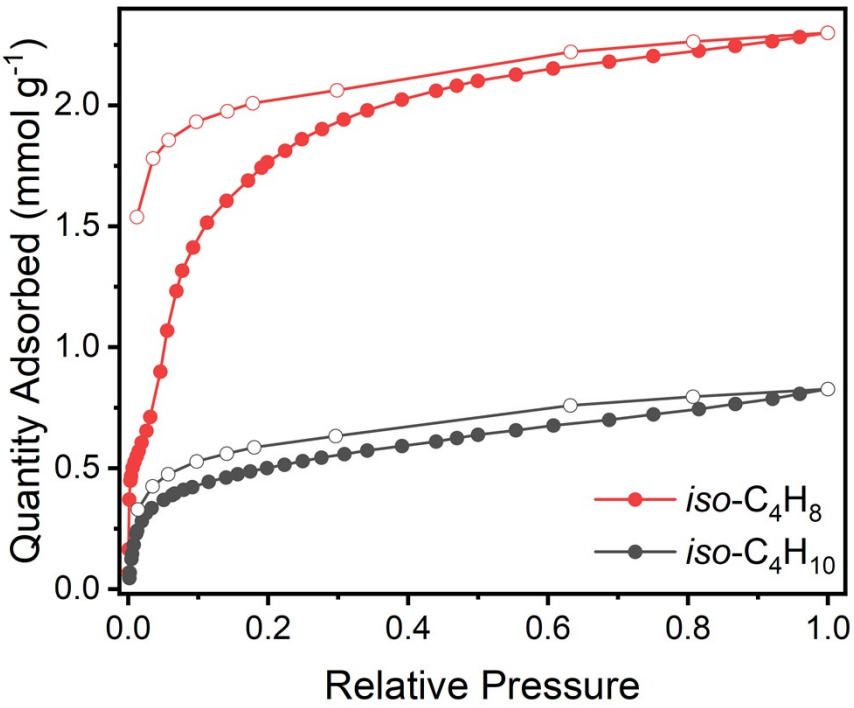

Fig. S8. The pure component adsorption and desorption isotherms of *iso*-C_4H_8 and *iso*-C_4H_{10} on ZU-603 at 298 K. (Solid circle, adsorption; empty circle, desorption)

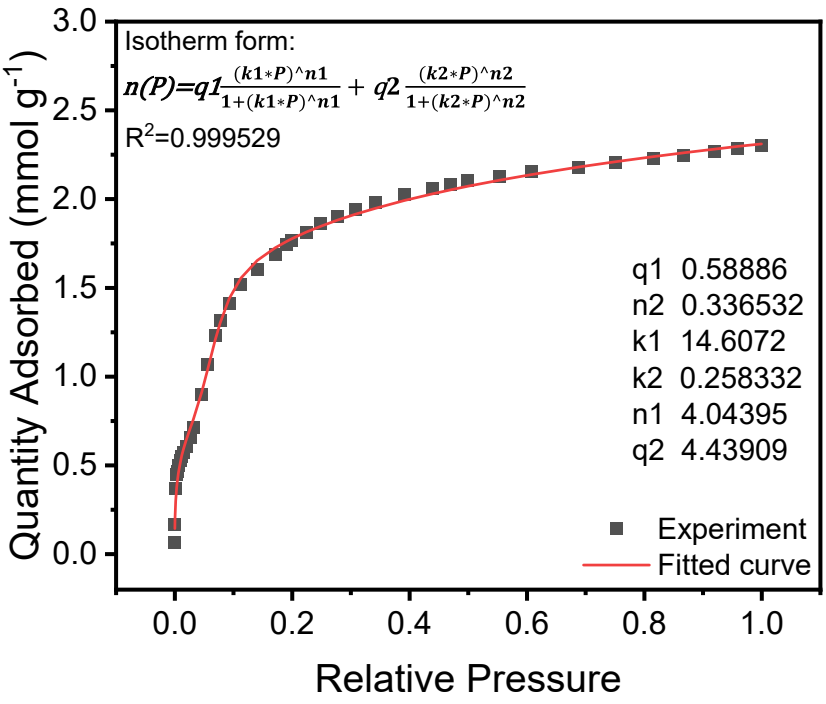

Fig. S9. DSLF fitting of the *iso*-C_4H_8 adsorption isotherm on ZU-603 at 298 K

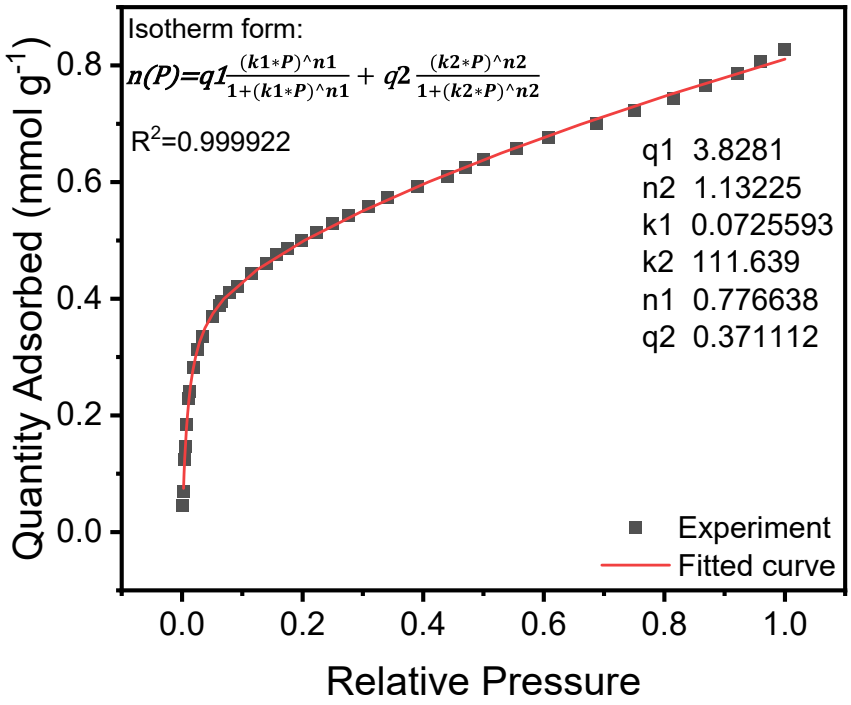

Fig. S10. DSLF fitting of the *iso*-C_4H_{10} adsorption isotherm on ZU-603 at 298 K

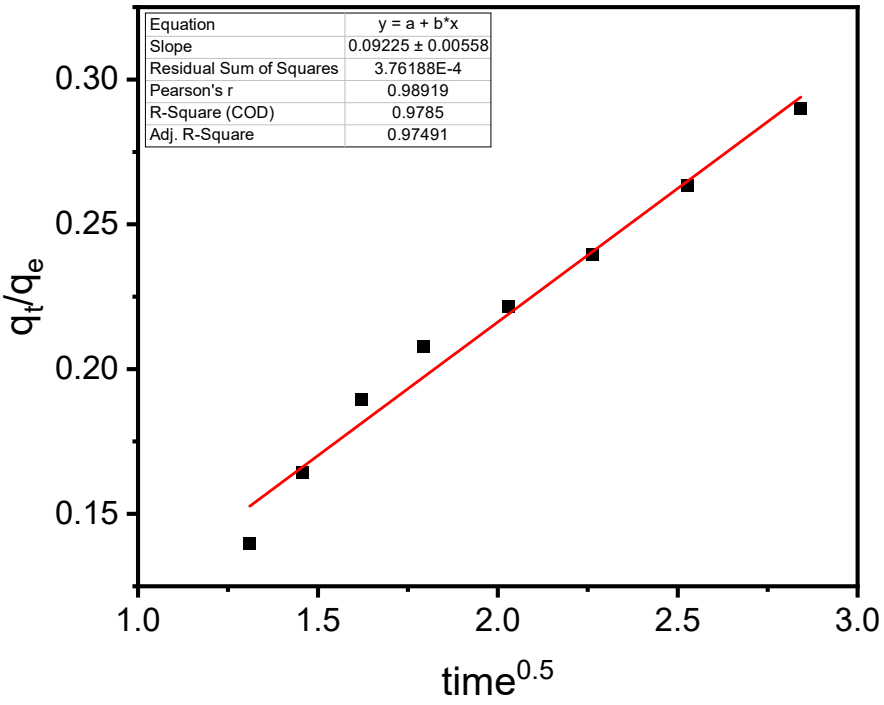

Fig. S11. Fitting of the time dependent adsorption profiles of *iso*-C_4H_8 on ZU-603 at 298 K using the micropore diffusion model.

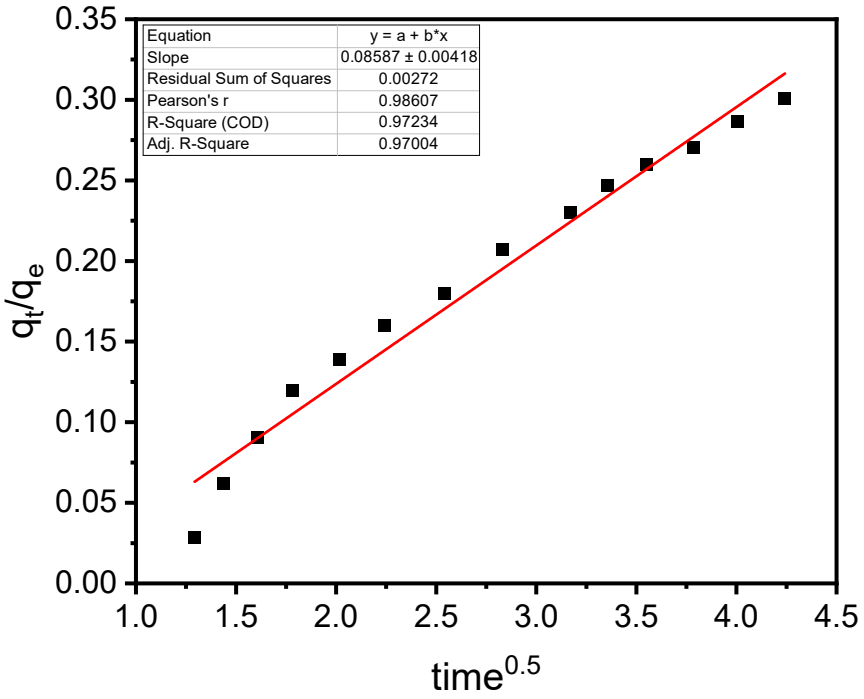

Fig. S12. Fitting of the time dependent adsorption profiles of *iso*-C_4H_8 on ZU-603 at 298 K using the micropore diffusion model.

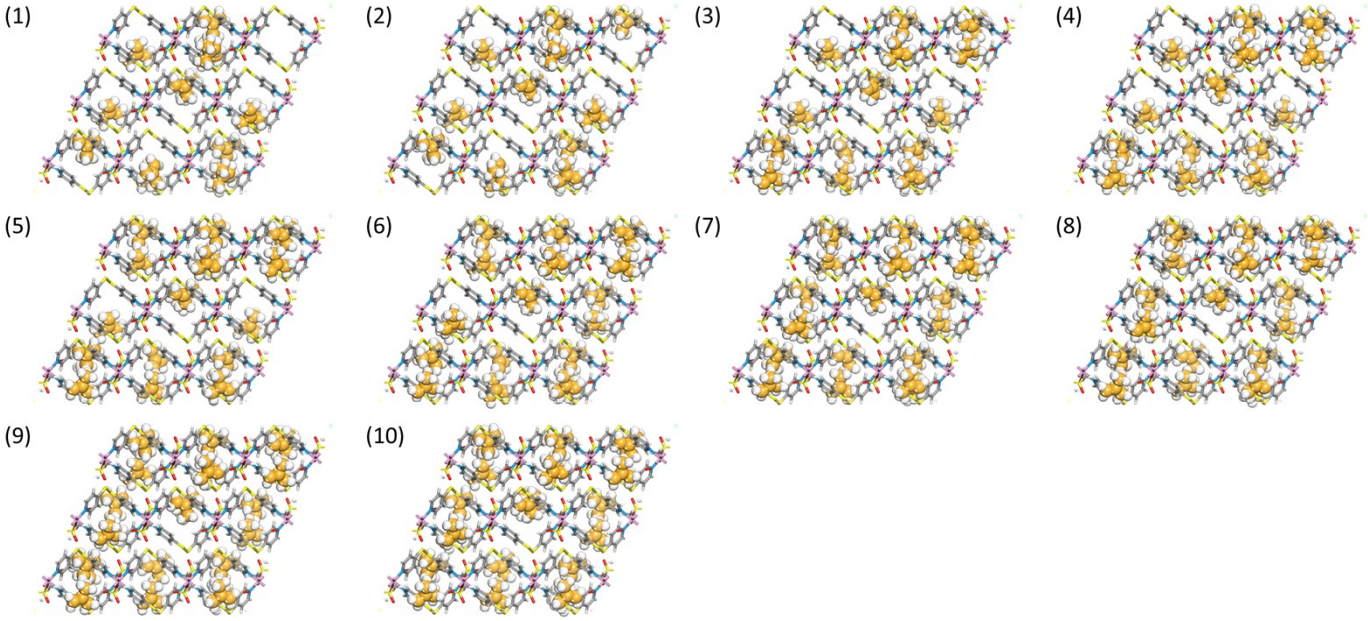

Fig. S13. Snapshots of GCMC simulations of *iso*-C_4H_8 adsorption on ZU-603 at 1 bar. Panels (1) to (10) illustrate increasing steps during the simulation.

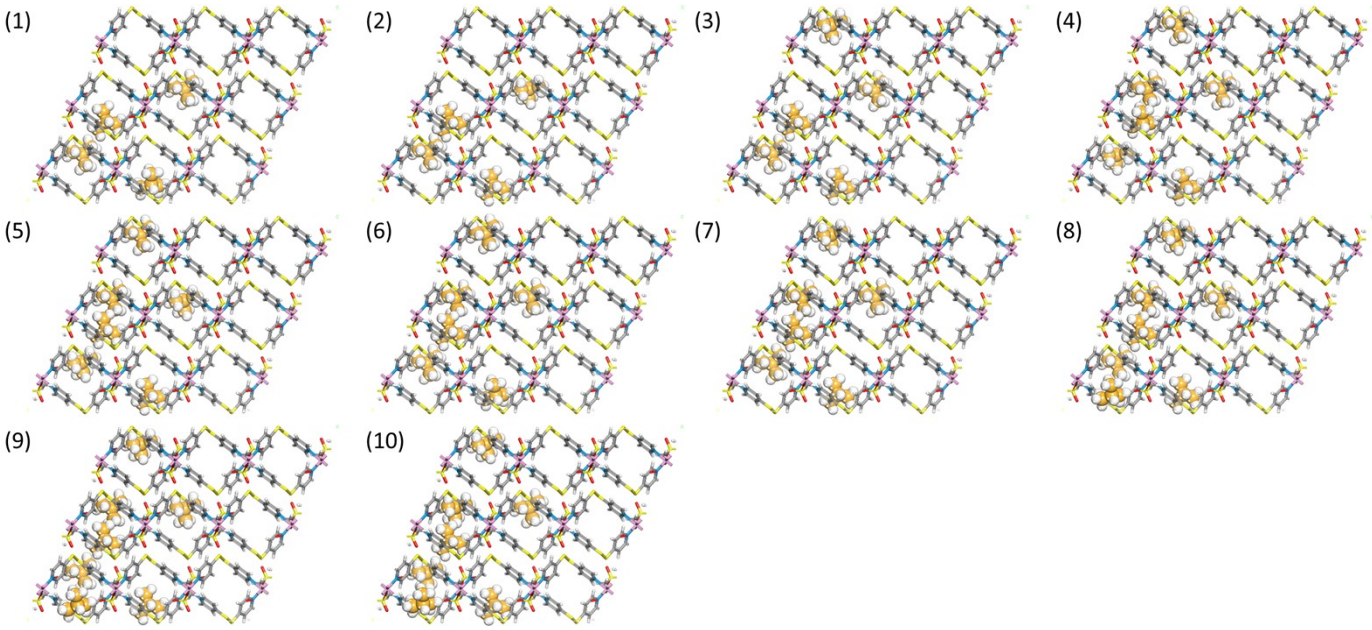

Fig. S14. Snapshots of GCMC simulations of *iso*-C_4H_{10} adsorption on ZU-603 at 1 bar. Panels (1) to (10) illustrate increasing steps during the simulation.

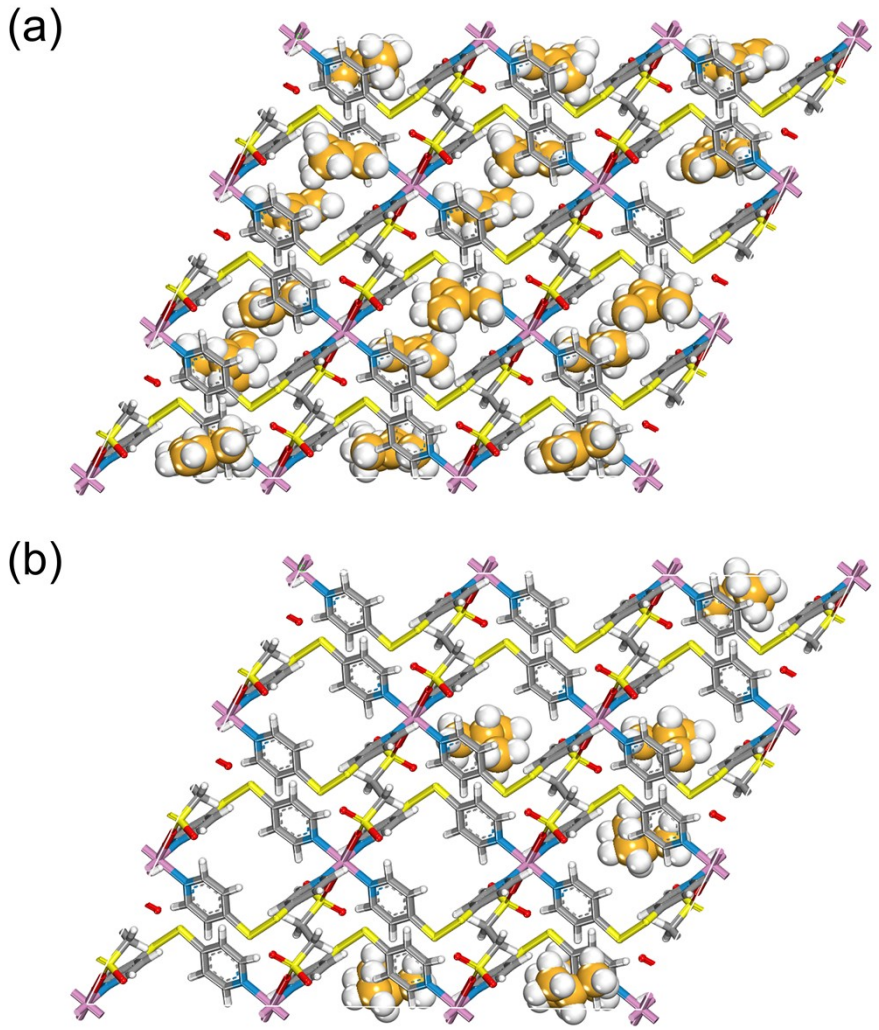

Fig. S15. Low energy snapshots of (a) *iso*-C_4H_8 and (b) *iso*-C_4H_{10} adsorption on ZU-603 at 1 bar.

Tables:

Table S1. Crystallographic data of activated ZU-603

Materials	ZU-603
Formula	C22H20CuN4O6S6
MW (g mol^{-1})	692.32
Crystal system	Triclinic
Space group	*P*1
a (Å)	9.7182(15)
b (Å)	10.6046(17)
c (Å)	10.6459(17)
α (°)	105.398(5)
β (°)	115.116(4)
γ (°)	105.493(5)
Volume ($Å^3$)	862.3(2)
Z	1
ρ (g cm^{-3})	1.333
μ (mm^{-1})	1.033
F (000)	353.0
Crystal size	0.12 × 0.11 × 0.06
Radiation	MoKα (λ = 0.71073)
2θ range for data collection (°)	4.766 to 57.554
Index ranges	$-13 \leq h \leq 13$, $-14 \leq k \leq 11$, $-13 \leq l \leq 14$
Reflections collected	8247
Independent reflections	4438 [R_{int} = 0.0356, R_{sigma} = 0.0581]
Data/restrains/parameters	4438/0/178
Goodness of fit on F^2	1.026
Final R indexes [I>=2σ(I)]	R1 = 0.0403, wR2 = 0.0946
Final R indexes [all data]	R1 = 0.0525, wR2 = 0.1015
Largest diff. peak/hole / e $Å^{-3}$	0.36/-0.55

Table S2. Separation performance comparison of different materials.

Materials	iso-C4H8	iso-C4H10	Uptake ratio
ZU-603	2.100	0.637	3.30
NI-GALLATE[1]	0.043	0.037	1.17
MG-GALLATE[1]	0.087	0.068	1.27
CO-GALLATE[1]	0.106	0.093	1.14
Mn-bpdc[2]	0.035	0.032	1.10
ZJNU-30a[3]	5.364	7.556	0.71
SD-65[4]	0.029	0.022	1.29
ZU-609[5]	0.106	0.088	1.20
HKUST-1[6]	6.851	5.583	1.23

References:

1. J. Chen, J. Wang, L. Guo, L. Li, Q. Yang, Z. Zhang, Y. Yang, Z. Bao and Q. Ren, Adsorptive Separation of Geometric Isomers of 2-Butene on Gallate-Based Metal–Organic Frameworks, *ACS Applied Materials & Interfaces*, 2020, **12**, 9609-9616.
2. W. Lu, H. Huang, Z. Hejin, C. Yanjiao, G. Xiangyu, Y. Fan and C. Zhong, Efficient separation of 1,3-butadiene from C4 hydrocarbons by flexible metal–organic framework with gate-opening effect, *AIChE Journal*, 2022, **68**, e17568.
3. H. Liu, Y. He, J. Jiao, D. Bai, D.-l. Chen, R. Krishna and B. Chen, A Porous Zirconium-Based Metal-Organic Framework with the Potential for the Separation of Butene Isomers, *Chemistry – A European Journal*, 2016, **22**, 14988-14997.
4. K. Kishida, Y. Okumura, Y. Watanabe, M. Mukoyoshi, S. Bracco, A. Comotti, P. Sozzani, S. Horike and S. Kitagawa, Recognition of 1,3-Butadiene by a Porous Coordination Polymer, *Angewandte Chemie International Edition*, 2016, **55**, 13784-13788.
5. J. Cui, Z. Qiu, Z. Yang, A. Jin, X. Cui, L. Yang and H. Xing, One-Step Butadiene Purification in a Sulfonate-Functionalized Metal–Organic Framework through Synergistic Separation Mechanism, *Angewandte Chemie International Edition*, 2024, **63**, e202403345.
6. M. Hartmann, S. Kunz, D. Himsl, O. Tangermann, S. Ernst and A. Wagener, Adsorptive Separation of Isobutene and Isobutane on Cu3(BTC)2, *Langmuir*, 2008, **24**, 8634-8642.